Bachmann, R., Glodny, J., Oncken, O., Seifert, W. (2009): Abandonment of the South Penninic-Austroalpine palaeosubduction zone, Central Alps, and shift from subduction erosion to accretion: constraints from Rb/Sr geochronology. - Journal of the Geological Society London, 166, 2, 217-231

DOI: 10.1144/0016-76492008-024.

Abandonment of the South Penninic-Austroalpine palaeo-subduction zone, Central Alps, and shift from subduction erosion to accretion: constraints from Rb/Sr geochronology

Raik Bachmann — Deutsches GeoForschungsZentrum (GFZ), Telegrafenberg, 14473 Potsdam, Germany. raik@gfz-potsdam.de
Present address: Horizon Energy Partners,
Prinses Margrietplantsoen 81, 2595 BR The Hague, The Netherlands
raik.bachmann@horizon-ep.com

Johannes Glodny — Deutsches GeoForschungsZentrum (GFZ), Telegrafenberg, 14473 Potsdam, Germany, glodnyj@gfz-potsdam.de

Onno Oncken — Deutsches GeoForschungsZentrum (GFZ), Telegrafenberg, 14473 Potsdam, Germany, oncken@gfz-potsdam.de

Wolfgang Seifert — Deutsches GeoForschungsZentrum (GFZ), Telegrafenberg, 14473 Potsdam, Germany, ws@gfz-potsdam.de

Corresponding author: Raik Bachmann

Abstract

We present new age data for the evolution of the suture zone between lower-plate South Penninic and upper-plate Austroalpine units in the Central European Alps. Rb/Sr deformation ages for mylonitized rocks of the South Penninic palaeo-subduction mélange and for deformed Austroalpine basement (Eastern Switzerland) shed light on the pre-Alpine and Alpine deformation history along the suture, as well as on syn-subduction interplate mass transfer. Rb/Sr age data define two age groups. The first group reflects pre-Alpine events within the upper plate basement, with varying degree of resetting by subsequent Alpine overprints. The second group marks the waning of subduction-related deformation along the South Penninic-Austroalpine suture zone, at around 50 Ma, and termination at ~47 Ma. Identical Rb/Sr ages for pervasively deformed Austroalpine and South Penninic lithologies point to tectonic erosion of the upper plate during subduction. We propose that underplating of the Middle Penninic micro-continent at ~50 Ma lead to the cessation of deformation within the South Penninic mélange, and shifted the zone of active deformation into the footwall. This also caused a contemporaneous upper plate surface uplift and shutoff of sedimentation in Alpine Gosau-type forearc basins.

In this study we provide the first time constraints for the end of subduction-related deformation along the suture zone between the Austroalpine nappe stack (hanging wall), and the South Penninic subduction mélange (footwall) in the European Central Alps. We investigated outcrops located in the eastern part of Switzerland (Fig. 1) along the fossil suture zone, and made use of the Rb/Sr system of white mica and coexisting phases (feldspar, apatite, calcite, epidote) in intensely deformed rocks from both tectonic units.

The here studied plate interface zone resulted from subduction of the South Penninic oceanic domain beneath the continental realm of the Adriatic plate (Austroalpine nappes) in the Cretaceous - Palaeogene (e.g. Froitzheim et al. 1996). Based on biostratigraphic data (Oberhauser 1983, Winkler & Bernoulli 1986), it was concluded that subduction here commenced in the mid Cretaceous, and that incipient involvement of the Middle Penninic micro-continent (Briançonnais) in the subduction process occurred in the Eocene (Ring et al. 1989). This entrance of continental crust may have lead to locking of the South Penninic – Austroalpine subduction zone in the Eocene, and to relocation of the site of subduction. However, solid age constraints on these processes are sparse up to now.
Large-scale differential tilting during exhumation of the fossil plate interface enables us to study this zone in present day outcrops, and provides access to various paleodepths (Figs. 1, 2). The exposed fossil plate interface has experienced flow and fracturing over an extended period of time, including minor overprint during Alpine continent-continent collision and subsequent exhumation. Nevertheless, we show that the fossil plate interface zone preserved its structural and isotopic record from the time when subduction-related deformation came to an end. It has to be pointed out that we consider only remnants of the South Penninic domain and the basal parts of the Austroalpine nappe stack as parts of the here studied fossil subduction plate interface. All other domains in the footwall of this zone, including the Middle Penninic and the North Penninic domains, do not belong to the here analyzed interface, as they were subducted beneath and accreted to the hangingwall later in the Alpine evolution, at a time when the South Penninic ocean was already closed. Therefore, subduction and accretion of these domains were accommodated by subsequently formed deformation zones in the footwall of the SSE-dipping South Penninic-Austroalpine plate interface (dip as inferred from the pattern of Late Cretaceous/Early Tertiary metamorphic isogrades, Fig. 2). Consequently, deformation and metamorphism for the Middle Penninic and North Penninic domains are expected to be younger in comparison to the deformation along the South Penninic-Austroalpine boundary zone.

Geological framework

Alpine evolution

The European Alps resulted, in their present form, from the collision of the European and the Adriatic continental plates, preceded by south-eastward to southward subduction and partial accretion of the intervening Penninic oceanic domain (Dewey et al. 1973, Platt et al. 1989, Stampfli et al. 1998, Rosenbaum & Lister 2005; Fig. 1). Most models differentiate between two ‘Alpine’ orogenic stages: A Cretaceous stage (referred to as ‘Eoalpine’, e.g., Wagreich 1995) is characterized by an east to southeast dipping subduction zone resulting in the closure of the Meliata ocean and leaving signatures of subduction-related deformation within the

Austroalpine nappes (belonging to the Adriatic plate, e.g. Schmid et al. 2004). Stacking within the Austroalpine units is associated with top-W, locally top-SW and top-NW thrusting (Ratschbacher 1986; Froitzheim et al. 1994, Handy 1996). The direction of convergence changed to roughly north – south during the Palaeogene orogenic stage (referred to as 'Mesoalpine' to 'Neoalpine', e.g., Wagreich 1995) with top-N thrusting and closure of the Alpine Tethys in between the European and Adriatic plates (Ratschbacher 1986; Froitzheim et al. 1994, Handy 1996, Schmid et al. 2004).

The oceanic Penninic units in between both continental realms (European and Adriatic plates, Fig. 1) were progressively subducted and deformed during convergent plate motion and partly accreted to the front and/or the base of the Adriatic plate. Palinspastic restoration of the Penninic units resulted in two separate oceanic basins divided by a micro-continent (e.g. Florineth & Froitzheim 1994, Schmid et al. 2004). This so-called Briançonnais terrane (or Middle Penninic unit) separated the northern basin (North Penninic or Valais ocean) from the southern basin (South Penninic or Piemont-Liguria ocean). Fragments from the Piemont-Liguria ocean experienced high pressure metamorphism in the Western Alps during the Palaeogene, whereas South Penninic units in the Eastern Alps are characterized by a Cretaceous to Paleogene tectonic imprint associated with variable grades of metamorphism ranging from diagenesis to blueschist facies (Dingeldey et al. 1997; Frey and Ferreiro Mählmann 1999, Schmid et al. 2004).

Geology of the working area and related regions

The working area is located in the Central Alps of Eastern Switzerland (Figs. 1, 2). The main geological units in the area belong to either the South Penninic or the Austroalpine domains. The Austroalpine domain overrode the South Penninic domain during Cretaceous/Palaeogene subduction (e.g. Ring et al. 1988, Schmid et al. 2004). Therefore, the immediate plate interface zone between the South Penninic domain (Arosa zone and the Platta nappe as its direct equivalent to the south (Biehler 1990), Fig. 2) and the Austroalpine represents a Late Cretaceous/Palaeogene continent-ocean suture (e.g. Handy 1996, Schmid et al. 2004) of a convergent plate margin. The large-scale structures of the Arosa zone are interpreted by Ring (1989) and Ring et al. (1988, 1989, 1990) as the deep parts of an accretionary wedge, formed at the tip of and below a thrust belt migrating towards the west. The apparent thickness of the South Penninic domain in the study area varies from a few tens of meters up to more than 2500 m.

Within the South Penninic domain, competent blocks of Austroalpine affinity (e.g., gneiss) and of South Penninic affinity (like pelagic cherts, and ophiolite fragments) are embedded in a less competent pervasively sheared matrix composed of serpentinites and calcareous shales (Deutsch 1983, Weissert & Bernoulli 1985, Ring et al. 1988, 1990). The South Penninic domain therefore can be described as a mélange, i.e., as an internally strained and fragmented complex containing rock fragments of various origin. Metamorphic conditions in the South Penninic domain range from upper diagenetic or lowermost greenschist facies in the north of the working area, to middle to upper greenschist facies in the southern parts (our own observations; Figs. 1, 2). The Austroalpine domain consists of a suite of gneissic to amphibolitic rocks which experienced pre-Alpine (mainly Permo-Carboniferous) and Early

(Eo-) Alpine deformation, overlain by and intercalated with variably deformed and metamorphosed Permo-Carboniferous clastic rocks, and Mesozoic sediments (e.g. Florineth & Froitzheim 1994, Ring et al. 1988, Manatschal et al. 2003).

The South Penninic-Austroalpine suture is best exposed in the here studied area of eastern Switzerland. Another, laterally equivalent exposure is found in the Valaisian Alps of southwestern Switzerland. Here, the Austroalpine Dent Blanche nappe (Fig. 1) is thrust upon Penninic (Piemonte) units of the Combin zone. The uppermost, South Penninic part (Tsaté nappe) of the Combin zone is an imbricated pile of metasediments and ophiolitic rocks with striking lithological similarity to the Arosa zone / Platta nappe. The Tsaté nappe is interpreted as being formed during closure of the South Penninic oceanic domain by subduction underneath the Austroalpine (Marthaler & Stampfli 1989, Stampfli & Marthaler 1990). Deformation fabrics in the Tsaté nappe reveal early top-NW shortening (Reddy et al. 2003). The metamorphic record is that of an early pressure-dominated, greenschist to blueschist facies metamorphism followed by intense greenschist facies overprint (e.g., Pfeiffer et al. 1991). In the Eastern Alps, a prominent location of exposure of the Austroalpine-Penninic suture is the edge of the Tauern Window (Fig. 1; Dingeldey et a. 1997; Schmid et al. 2004).

Subduction channel concept

Following Ring et al. (1988, 1990), the South Penninic domain (Arosa zone and Platta nappe) in our study area represents the deep parts of a subduction complex, i.e., of an accretionary wedge. With its internal structure of a mélange, the South Penninic domain therefore is best interpreted as a subduction mélange, formed in a subduction channel. Cloos & Shreve (1988 a, b) have introduced the subduction channel concept denoting a shear zone of variable width between the upper and lower plates of convergent margins. Within the subduction channel, material from both plates is intermingled and transported downwards. The channel material may then either get lost into the Earths’ mantle, it may be partly accreted to the front of a growing accretionary wedge (frontal accretion), or accreted to the base of the hanging wall (basal accretion) (von Huene & Scholl 1991). Material may also be removed from the tip (frontal tectonic erosion; Vannucchi et al. 2008) or from the base of the upper plate (basal tectonic erosion; e.g. Clift and Vannucchi 2004). In the case of the South Penninic subduction melange (Arosa zone / Platta nappe), the downgoing plate has been oceanic in nature, and the overriding Austroalpine dominantly consists of continental lithologies. In such a situation of contrasting lithofacies, abundance and lithology of clasts within the matrix of the subduction mélange can be used to infer prevalence of either tectonic erosion, or accretion (Oncken 1998).

Structural aspects of the fossil plate interface zone

We measured tectonic features like foliation, stretching lineations, shear bands, tension gashes, folds, and faults, and assessed their relative age relationships in a series of profiles across the plate interface, sampling different palaeo-depths of the palaeo-subduction zone (Figs. 2, 3). The South Penninic mélange close to the contact to the Austroalpine hanging wall experienced a penetrative deformation with foliation planes dipping moderately towards SE to NE and associated stretching lineations plunging smoothly between SE and ENE (Fig. 3).

These structures are best developed in the south of the working area. Deformation of the South Penninic mélange increases towards the south of the working area. This is expressed by a more distinct and tighter foliation, and by the progressive obliteration of pre-existing sedimentary structures. Shear sense indicators embedded in this penetrative foliation (e.g., rotated clasts, shear bands) change gradually from top-NW in the north of the working area via top-W in the central parts to top-SW in the southernmost parts. The variation in the observed kinematic indicators may either be the result of oblique subduction, which favours partitioning of strain (Beck 1983, Beck Jr. 1991, Robin and Cruden 1994), or of lateral changes of the end of deformation during a progressive change of subduction kinematics.

Deformation of the Austroalpine nappe stack is reflected by microscale fracture zones reactivating the pre-existing gneissic foliation of probably Variscan age in the northern part of the working area. This overprint increases towards the south, as indicated by more and more intense growth and recrystallization of fine-grained sheet silicates parallel to the pre-existing foliation. Orientation of foliation in the Austroalpine rocks parallels the corresponding foliation within the South Penninic mélange, at least in the first few hundred meters above the base of the hanging wall. Orientations of structural features are similar in both the South Penninic mélange and the basal parts of the Austroalpine domain (Fig. 3). Based on these results, we infer a general top-W motion of the hangingwall. This sense of shear is fairly consistent with the Paleocene to Eocene SE-ward subduction of Penninic units beneath the advancing Austroalpine orogenic wedge inferred from paleogeographic reconstructions (Stampfli et al. 1998; see review in Rosenbaum & Lister 2005). It also conforms with top-NW shear sense indicators at the Penninic-Austroalpine interface along the Dent Blanche nappe, SW Switzerland (Reddy et al. 2003).

Subsequent localized deformation with significantly lower intensity overprints the above described penetrative fabric in both units. However, a complete erasure of the pervasive fabric in both the South Penninic mélange and the Austroalpine domain by younger deformational processes is nowhere observed (see also Ring 1989, Dürr 1992). The main late feature is a superimposed set of brittle-ductile shear bands indicating top-E to top-SE directed tectonic transport, a feature becoming more prominent towards the south (Fig. 3). All the above structures are overprinted by large-scale, roughly E-W oriented open folds (Fig. 3).

Published age data

Time constraints on the evolution of the South Penninic mélange are sparse. The few existing data are summarized below; an overview is given in Fig. 4. Oceanic spreading, and thus opening of the South Penninic ocean, is dated in the Eastern Alps to have occurred at least since the Early to Middle Jurassic (186 ± 2 Ma, Ar/Ar on biotite, Ratschbacher et al. 2004). For the Western Alps, the sedimentation history (Baumgartner 1987) and isotopic ages (Rubatto et al. 1998; Gebauer 1999) point to oceanic spreading between ~185 and 155 Ma. According to Wagreich (2001, and references therein), the transition to an overall convergent setting and the initiation of oblique, roughly south-eastward subduction of the Penninic domain beneath the Austroalpine occurred during the Aptian/Albian, at ~110 Ma. This is supported by high-pressure detrital minerals found in ophiolite-rich flysch deposits from the South Penninic domain, which show ages ranging between 120 to 100 Ma (see overview in

Handy and Oberhänsli, 2004). Onset of subduction in Abtian / Albian times is also consistent with sedimentological and biostratigraphic constraints. Latest sedimentation within the Arosa zone (South Penninic) is documented to have occurred within the Early Coniacian, at ~90 Ma (Late Cretaceous, Ring 1989). Flysch deposits from the Platta nappe (South Penninic) show sedimentation ages ranging from Aptian to Albian (late Early Cretaceous; Ring 1989). Overall, no sediments younger than ~90 Ma are known from the South Penninic mélange, and subduction-related deformation may have been on the way at that time.

For the subduction of the South Penninic melange underneath the Austroalpine Dent Blanche nappe (SW Switzerland), a Rb/Sr deformation age of ~48 Ma has been interpreted to reflect the final stages of top-NW thrusting of the Austroalpine over the mélange (Reddy et al. 2003). In the Eastern Alps, ^{40}Ar-^{39}Ar data around 55 to 50 Ma for white mica from the Austroalpine-Penninic interface in the northeastern Tauern Window were determined by Liu et al. 2001. Combined with similar ^{40}Ar-^{39}Ar whole rock ages around 50 Ma for schists from the northwestern edge of the Tauern Window (Dingeldey et al. 1997), these data point to emplacement of the Austroalpine onto Penninic units in the Tauern Window region around 50 Ma.

Relocation of the active subduction zone into structurally lower, Middle and North Penninic units, respectively the foreland (i.e. towards NW in modern coordinates; Fig. 4), is indicated by isotopic ages between ~52 Ma and ~30 Ma for units exposed in the footwall of South Penninic units in the Western and Central Alps (Markley et al. 1998, Cartwright and Barnicoat 2002, Reddy et al. 2003, Meffan-Main et al. 2004; Rosenbaum & Lister 2005, and references therein). This age interval for subduction is again consistent with the sedimentation history. Flysch deposits comprising the footwall of the South Penninic mélange (derived from Middle and North Penninic units, and from the distal European margin, Figs. 2, 4) range in age from Early Cretaceous to Early/ Middle Eocene (Trautwein et al. 2001). Stampfli et al. (2002) reported distal flysch deposition until 43 Ma. Therefore, at least parts of the subduction history of Middle- and North Penninic units must postdate 43 Ma.

Rb-Sr dating of deformation: Methodology

For the purpose of Rb/Sr isotopic dating we used the internal mineral isochron approach (Glodny et al. 2002, 2005). Sample selection was based on thin section observations, combined with sample-specific structural evidence from the field. Wherever viable we selected samples of small size (approximately 20 – 100 g), texturally exclusively recording a single, distinct, recrystallization-inducing tectonic and metamorphic event. In our study this is the general top-W directed tectonic transport within the South Penninic mélange and the basal parts of the Austroalpine domain. We focused on samples containing white mica as a high Rb/Sr phase. The Rb/Sr isotope system of white mica is thermally stable to temperatures higher than 500°C – 550°C, but may be fully reset by dynamic recrystallization even at lower temperature (Inger & Cliff 1994, Freeman et al. 1997, Villa 1998). According to Müller et al. (1999), isotopic reequilibration between white mica and coexisting phases during mylonitization may occur at temperatures as low as 350°C. Careful study of the correlation between microtextures and isotopic signatures, both by conventional mineral separation techniques (Müller et al. 1999, Glodny et al. 2008) and Rb/Sr microsampling (Müller et al. 2000, Cliff & Meffan-Main 2003) has shown that complete synkinematic recrystallization in mylonites is usually accompanied by isotopic reequilibration. Therefore, Rb/Sr isotopic data from penetratively deformed rocks can be used to date the waning stages of mylonitic deformation, given that deformation occurred below the temperature range for diffusional resetting. In our samples, deformation and related white mica recrystallization occurred at temperatures well below 500°C to 550°C, which makes sure that Rb/Sr isotopic signatures record dynamic recrystallization. To detect possible Sr isotope inhomogeneities resulting from isotopic inheritance, from long-term or incomplete dynamic recrystallization, from diffusional Sr redistribution, and/or from alteration processes, white mica was analysed in several, physically different (in terms of magnetic properties and/or grain size) fractions wherever possible. According to Müller et al. (1999) this approach ensures control on the possible presence of unequilibrated, pre-deformational white mica relics. In addition, mineral concentrates of feldspar, apatite, calcite, and epidote were produced. Care was taken to exclude material altered by weathering or by late fluid-rock interaction. White mica concentrates were ground in ethanol in an agate mortar, and then sieved in ethanol to obtain pure, inclusion-free separates. All mineral separates were checked, and finally purified by hand-picking under a binocular microscope. Rb and Sr concentrations were determined by isotope dilution using mixed $^{87}Rb/^{84}Sr$ spikes. Determinations of Rb and Sr isotope ratios were carried out by thermal ionization mass spectrometry (TIMS) on a VG Sector 54 instrument (GeoForschungsZentrum Potsdam). Sr was analyzed in dynamic multicollector mode. The value obtained for $^{87}Sr/^{86}Sr$ of NBS standard SRM 987 was 0.710268 ± 0.000015 (n = 19). The observed Rb isotopic ratios were corrected for 0.25% per a.m.u. mass fractionation. Total procedural blanks were consistently below 0.15 ng for both Rb and Sr. Because of generally low and highly variable blank values, no blank correction was applied. Isochron parameters were calculated using the Isoplot/Ex program of Ludwig (1999). Decay constants are those recommended by Steiger & Jäger (1977). Standard errors of ± 0.005% for $^{87}Sr/^{86}Sr$ ratios and of ±1.5% for Rb/Sr ratios, as derived from replicate analyses of spiked white mica samples, were applied in isochron age calculations (cf. Kullerud 1991). Individual analytical errors were generally smaller than these values. Rb/Sr analytical data are given in Table 1. All analytical uncertainties are reported at the 2σ confidence level throughout this paper.

Petrography and sampling

The South Penninic subduction mélange exhibits a N-S gradient in metamorphic conditions. In the northern part of the working area, Alpine metamorphism did not exceed diagenetic grade to lower greenschist facies. In the southern part, rocks of the mélange as well as the basal parts of the Austroalpine nappe stack were metamorphosed at middle to upper greenschist-facies conditions during Alpine orogeny. This is inferred from dynamic recrystallization fabrics in quartzite and synkinematic quartz veins, as well as from Si contents in phengitic white mica (Table 2). Along the N-S profile, we sampled calcsilicates, calcmylonites, quartz-mica schists and a quartz-rich metamorphic mobilisate from the South Penninic mélange, as well as quartz mylonites, mylonitized Permian meta-volcanics and quartz-mica schists from the basal parts of the Austroalpine nappe stack (Figs. 5a-f). Samples used for Rb/Sr dating are fine grained, strongly foliated or mylonitized, with the exception of the quartz mobilisate. Minerals found in these rocks include quartz, feldspar, white mica, biotite, calcite, apatite, opaque minerals, and epidote. Locally, retrograde chlorite occurs. The mineral assemblages in general testify to greenschist-facies conditions during deformation in both the South Penninic subduction mélange and in the basal parts of the Austroalpine. The strong deformation (Figs. 5d, e) caused, in most samples, optically complete to nearly complete recrystallization of white mica, apatite, calcite, and albite. Samples were selected to exclusively show a general top-W direction of tectonic transport (Fig. 3), or only very minor later overprints. Sample locations are shown in Figure 6. Petrographic descriptions are summarized in Table 2. To sum up, the samples selected for Rb/Sr isotopic dating yield very similar metamorphic conditions (middle to upper greenschist grade, as far as it can be constrained by the generally 'simple' paragenesis), kinematic indicators (generally top-W) and microstructures (quartz showing bulging and subgrain rotation recrystallization, strongly aligned minerals within the calcmylonites) for both the base of the upper plate Austroalpine domain and the South Penninic subduction mélange.

Results

Rb/Sr data

We obtained well-defined isochron ages for three samples from the southern part of the working area, originating both from the basal parts of the Austroalpine domain and the South Penninic mélange. Sample C-15 (quartz mica schist, Fig. 5d, profile 6 in Fig. 6, South Penninic mélange) yielded a four-point isochron age of 53.85 Ma ± 0.59 Ma (Fig. 7a). Sample B-11 (quartz rich mylonite, Figs. 5c, 5e; profile 7 in Fig. 6, Austroalpine) yielded a five-point isochron age of 48.6 Ma ± 0.7 Ma (Fig. 7b). The five-point isochron of sample B-32 (calcsilicate, profile 7, South Penninic mélange) resulted in a slightly younger age of 47.1 ± 0.4 Ma (Fig. 7c). Additionally, for five samples from the upper plate and the South Penninic mélange, as well as for a quartz mobilisate we obtained correlations in Rb/Sr isochron plots which reveal minor apparent initial isotopic disequilibria between the analyzed mineral fractions (evident from elevated MSWD values of regression) (Figs. 7d-h). Nevertheless, these samples give good hints on the age of their last important overprint. Sample C-5 (Permian meta-volcanic rock, profile 5, Austroalpine) resulted in an age of 48.3 Ma ± 9.3 Ma, based on a five-point correlation (Fig. 7d). A six-point data array for sample C-12 (quartz mica schist, profile 6, Austroalpine) yielded an age value of 59.9 Ma ± 3.4 Ma (Fig. 7e). The quartz mobilisate B-8 (Fig. 5a, profile 7 in Fig. 6, South Penninic mélange) resulted in a correlation based on five points corresponding to an age of 49.2 Ma ± 8.6 Ma (Fig. 7f). For sample B-13 (quartz mica schist, profile 7, South Penninic mélange), a five-point regression resulted in an age of 57.7 ± 4.9 Ma (Fig. 7g). A four-point correlation was obtained for sample B-14 (calcmylonite, Fig. 5b, profile 7 in Fig. 6, South Penninic mélange) corresponding to an age of 54.2 Ma ± 1.3 Ma (Fig. 7h). In summary, there is a clear signal for a deformation process waning at around 50 Ma, and termination of all deformation at ~47 Ma.

We farther obtained Rb/Sr mineral data pointing to considerably older, pre-Cretaceous events for some samples from the base of the crystalline upper plate (Austroalpine) in the northern part of the working area (Figs. 8a-c). These samples are all characterized by Sr-isotopic disequilibria. Disequilibria are probably related to incomplete resetting of the mineral isotope systems due to incomplete deformation-induced recrystallization during younger overprints, for which indications are visible in thin sections (Fig. 5f, sample J91). For sample 4d (mylonite, profile 1, the northernmost sample) regression of five Rb/Sr mineral data yielded 303 Ma ± 17 Ma (Fig. 8a). Sample 10c (mylonitic shear zone, profile 2) yields an apparent age of 175 Ma ± 28 Ma (n = 4, MSWD = 54, excl. apatite; Fig. 8b). For sample J91 (gneiss, profile 4), regression of seven mineral data pairs points to an apparent age of 192 Ma ± 30 Ma (Fig. 8c).

Discussion

Rb/Sr ages: pre-Eocene signatures

The analyses of Rb/Sr data for the different samples resulted in 2 age groups, despite the fact that all samples recorded apparent top-W tectonic transport. The first group is exclusively comprised of samples from the base of the hanging wall Austroalpine nappe stack. Here, the oldest apparent age of 303 ± 17 Ma (sample 4d, Fig. 8) is within the range of 'Variscan' ages known from the Austroalpine of this region (cf. Thöni 1999 for review), while the data for sample J91 (disequilibria; poorly constrained apparent age of 192 ± 30 Ma, Fig. 8) might reflect partial resetting of pre-Alpine signatures, probably by Alpine-age overprints. The fact that the apparently 'younger' sample originates from a more southern (deeper) position along the fossil plate interface is consistent with the observed increasing intensity of Alpine imprints on textures and mineral assemblages towards the South. This observation points to more effective resetting of the isotope system by deformation at higher metamorphic conditions. Sample 10c from a mylonitic shear zone within the upper plate resulted in an age of 175 ± 28 Ma (Fig. 8). It remains unclear whether this (biotite-based) age value may date any distinct Jurassic deformation event within the Austroalpine, or whether it similarly reflects partial isotopic resetting during Alpine overprint.

Eocene deformation

A number of samples from both the base of the Austroalpine nappe stack and the South Penninic mélange in the southern part of the working area, resulted in a second group of ages, around 50 Ma (Fig. 9). For the samples from the basal parts of the upper plate we interpret these ages to reflect the final stages of mylonitization-related isotopic reequilibration related to penetrative Alpine deformation, under greenschist grade conditions. There is a striking similarity between the deformation ages calculated for the basal parts of the upper plate, and for the South Penninic mélange, in the southern part of the study area (Fig. 9). We therefore interpret the ages obtained for the South Penninic mélange to reflect the same deformation-induced recrystallization as observed in the samples from the base of the Austroalpine. It appears that deformation along the plate interface zone between the South Penninic mélange and the Austroalpine occurred (and ceased) over a prolonged period, at least over a time span bracketed by our isochron age data (53.85 ± 0.59 Ma to 47.1 ± 0.4 Ma). Possibly, even somewhat earlier increments of deformation are recorded by the samples C-12 (Fig. 7) and B-13 (Fig. 7). These samples show higher apparent ages (59.9 ± 3.4 and 57.7 ± 4.9 Ma, respectively), combined with positive correlations between white mica grain sizes and apparent ages (e.g. sample B-13: large white mica crystals plotting above, and smaller white micas below the regression line, Fig. 7). This grain size – age correlation reflects some kind of isotopic inheritance. The correlation is consistent with protracted deformation, with incomplete isotopic resetting of early-recrystallized grains during the latest stages of deformation. Finally, there is no hint in the dataset to any ductile overprint postdating the Lower Eocene (~50 Ma) record of waning deformation. The dated foliation-parallel prograde metamorphic mobilisate (sample B-8) resulted in an (imprecisely constrained) apparent age of 49.2 ± 8.6 Ma (Fig. 7), pointing to the activity of fluids along the active palaeo-subduction zone.

Material accreted to the base of the South Penninic subduction mélange (i.e. the Middle Penninic domain) yields synkinematic white mica ages systematically younger than 52-48 Ma (Thöni 1981, Thöni 1988, Markley et al. 1998, Cartwright and Barnicoat 2002, Reddy et al. 2003, Meffan-Main et al. 2004; Rosenbaum & Lister 2005, and references therein), indicating that subduction-related deformation had already shifted into the footwall of the South Penninic subduction mélange at about 48 Ma (Fig. 9). It has been proposed before that incipient subduction of continental Penninic material (most likely the Middle Penninic micro-continent) occurred in the early Eocene, in a time span between 55 Ma and 45 Ma (e.g., Ring et al. 1989, von Blanckenburg & Davies 1995). Our Rb/Sr age data are in line with these suggestions. Our results clearly constrain the end of deformation along the South Penninic-Austroalpine suture zone to between ~54 and ~47 Ma, consistent with the locking of the South Penninic subduction zone by the incoming Middle Penninic micro-continent (e.g., Froitzheim et al. 2003). This process most likely transferred the zone of active deformation further into the footwall, leaving the South Penninic paleo-subduction mélange as a part of the upper plate, which subsequently overrode the Middle Penninic domain. In summary, our Rb/Sr isotopic data provide the first precise geochronological constraints on the end of subduction related deformation along the South Penninic-Austroalpine suture zone in the Eastern Swiss Alps, i.e. on the abandonment of this palaeo-subduction interface.

This age constraint is in line with results of Dingeldey et al. (1997) and Liu et al. (2001), which provide ^{40}Ar-^{39}Ar ages around 55-50 Ma for Austroalpine-Penninic interface units in the Tauern window area. These data can similarly be interpreted as dating the locking of this paleosubduction zone. The age constraint also conforms with the interpretation of the oldest age for top-NW deformation from the footwall of the Dent Blanche Nappe, SW Switzerland, as dating final overthrusting of the Austroalpine here at ~48 Ma (Reddy et al. 2003). Consistency between isotopic ages for abandonment of the Austroalpine-South Penninic suture zone between the Western Alps, the Eastern Alps and our study area suggests a near-synchronous Early Eocene termination of subduction of the South Penninic ocean along the evolving Alpine orogenic belt. In other words, at that time the Alps evolved as a more or less cylindrical orogen.

It has to be stressed that the structural and geochronologic record of a subduction channel is persistently renewed, in response to processes such as sediment subduction, deformation, and tectonic erosion. Only when material finally leaves the active parts of the subduction channel by accretion to the base of the hanging wall, the deformation structures and the geochronologic record can be preserved. Deformation-induced isotopic resetting during accretion of material to the base of the upper plate is caused by permanent strain accumulation, due to the velocity gradient between the lower and upper plates. Depending on the degree of strain localization in the zone between both plates, deformation and consequently a zone of deformation-induced isotopic resetting may even penetrate into the base of the overriding plate. As outlined above, we interpret our Rb/Sr age data as dating the end of deformation within the here analyzed parts of the paleo-subduction channel, and consequently as constraining the abandonment of the South Penninic-Austroalpine suture zone at around 50 Ma.

Abandonment of the palaeo-subduction zone – hints from Gosau group sediments

Sedimentary basins, collectively known as 'Gosau-type' basins (Fig. 1) developed as slope basins along the northward deepening slope of the Adriatic plate at the front of the orogenic wedge (Wagreich 1991, 1995, Wagreich & Krenmayr 2005). Early, Aptian to Lower Cenomanian piggyback basins were formed on the evolving Cretaceous orogenic wedge of the Eastern Alps (Wagreich 2001). A second type of basins, the Gosau basins *sensu strictu*, are extension-related and can be described as collapse basins. They represent synorogenic sedimentation along a broad transform zone, and are interpreted as the consequence of oblique subduction of the South Penninic ocean underneath the Austroalpine nappe stack with dextral transtension and strike-slip faulting (Wagreich and Decker 2001, Wagreich and Krenmayr 2005). The Gosau basins comprise a stratigraphic record from the Upper Turonian to the early Eocene, evolving from terrestrial and shallow marine deposits into deep marine sediments. Following Wagreich (1991, 1993), development of the Gosau basins is driven by tectonic erosion, causing a large scale subsidence pulse during the Late Cretaceous. Subsidence and sedimentation continued until the Eocene.

There is a striking similarity between our new Rb/Sr deformation ages for the abandonment of the South Penninic palaeo-subduction interface, and the timing of the end of subsidence and sedimentation within the Gosau group depocenters (Wagreich 1995), both at around 50 Ma (Eocene), suggesting a causal relationship. According to Wagreich (1995) the termination of the Gosau group sedimentation is associated with the end of tectonic erosion and the transformation of the erosive margin again into an accretive one. We suggest that tectonic underplating and wedge thickening from accretion of the Middle Penninic micro-continent, roughly at 50 Ma (e.g. Ring et al. 1989, von Blanckenburg & Davies 1995, Froitzheim et al. 2003), accounts for both the locking of the South Penninic subduction zone and the associated termination of tectonically erosive mass transfer mode. Such accretive underplating may have resulted in the termination of Gosau group sedimentation due to an accretion-related pulse of uplift.

Isotopic dating – a hint for mass transfer mode

The systematics of our Rb/Sr isotopic age data for the South Penninic paleosubduction zone provide hints for the temporal evolution of mass transfer within fossil subduction systems in general. As illustrated in Figure 10 (a, b, c), hypothetical endmember scenarios for mass transfer mode within subduction channels comprise: 1) continuous underplating (addition of material to the base of the upper plate, i.e. basal accretion) (Fig. 10a), 2) continuous tectonic erosion removing material from the base of the upper plate (Fig. 10c), or 3) steady state, in a sense of continuous material flow neither adding nor removing material (Fig. 10b). For the isotopic record of deformation-sensitive isotopic systems in such endmember scenarios, the following predictions can be made:

Scenario a): A case scenario of continuous underplating at an accretive margin (Fig. 10a) would result in a distinct trend of isotopic ages within the upper plate. The ages recorded in the upper plate accretionary complex would get systematically younger with depth, towards the subduction channel (e.g. Glodny et al. 2005). No major breaks in the isotopic age record are expected, neither between the subduction channel and its immediate hangingwall, nor within the hangingwall accretionary complex. Lithologically discernible clasts of upper plate material would be rare or absent within the subduction mélange.

Scenario b): In the case of steady-state (continuous) material flow, isotopic ages for the upper plate would reflect the pre-subduction geological history, possibly with a domain of partial, subduction-related reset of age information at the base of the upper plate. A clear contrast between deformation ages from the subduction mélange (reflecting the latest stage of deformation), and the upper plate age record is expected (Fig. 10b). Continuous material flow within the subduction channel would constantly reset the isotopic systems here, until final shutdown of ductile deformation.

Scenario c): Continuous tectonic erosion would result in nearly identical isotopic ages for both the deformed basal parts of the upper plate and the subduction mélange. This would be due to ongoing mobilization of material at the base of the upper plate followed by tectonic downdip removal, which persistently shifts the region of deformation-induced isotopic resetting into the upper plate (Fig. 10c). A distinct break in recorded isotopic ages is expected just above the zone of subduction-related ductile deformation. This isotopic record would be connected to the presence of clasts of upper plate material within the subduction mélange.

Our Rb/Sr isotopic data are roughly identical for both the basal parts of the Austroalpine upper plate and the South Penninic subduction mélange at around 50 Ma (Fig. 9). Referring to the endmember scenarios above, this favours either steady state material flow (Fig. 10b) or tectonic erosion (Fig. 10c) as the possible material transfer modes active within the subduction channel until the time of abandonment of this major suture zone. Based on the observation of numerous upper plate clasts embedded within the subduction mélange, we conclude that tectonic erosion was the main material transfer mode along the plate interface zone prior to about 50 Ma. This is in line with the postulation by Wagreich (1991, 1993, 1995) that tectonic subduction erosion has driven the formation of the Gosau basins.

As demonstrated with this example, precise studies of the isotopic record of fossil subduction complexes have the potential to constrain the long term evolution of mass transfer in terms of tectonic erosion, basal accretion and steady state material flow.

Conclusions

We present the first precise Rb/Sr age data for the termination of subduction-related deformation along the South Penninic-Austroalpine suture zone in the Eastern Swiss Alps. Beside some relics from pre-Alpine events in the Austroalpine, we found ages consistently around 50 Ma both in the subduction mélange and the overlying Austroalpine, interpreted to reflect recrystallization in both units in response to late increments of deformation along the palaeo-subduction interface. A ~50 Ma metamorphic quartz mobilisate points to syn-subductional dehydration, fluid activity and mineral precipitation. The dated waning of deformation along the palaeo-subduction interface is inferred to be due to final basal accretion of the former subduction channel material to the upper plate. Deformation finally ceased at ~47 Ma. According to our structural data, the latest increments of deformation at ~50 Ma are characterized by a roughly top-W to NW direction of tectonic transport. Referring to published paleogeographic reconstructions, the end of subduction-related deformation is best explained by the locking of the South Penninic palaeo-subduction interface due to underplating of the Middle Penninic micro-continent, a process that caused a relocation of convergence-related strain from the palaeo-subduction mélange into the new, Middle Penninic footwall. It appears that this final closure of the South Penninic ocean occurred in a cylindrical mode, nearly simultaneous along the evolving Early Eocene Alpine orogen. The shutoff of sedimentation in the forearc Gosau basins is contemporaneous with basal accretion of the South Penninic mélange due to incipient subduction of Middle Penninic units, both processes occurring in the early Eocene (~50 Ma). We hypothesize a causal link between the two events, with the change from tectonic erosion to basal accretion being responsible for a regional pulse of uplift, leading to inversion of the forearc basins.

We propose that the mass transfer mode of a palaeo-subduction system can be constrained using the combined deformation age record of both the upper plate and the subduction channel mélange, together with the lithological record of the subduction mélange. In our case, combined evidence from identical Rb/Sr ages for the deformed lowermost part of the Austroalpine and for the South Penninic subduction mélange, from the abundance of upper plate clasts in the subduction mélange, and from the syn-subduction evolution of Gosau forearc basins, points to tectonic erosion as the prevailing mass transfer mode at least during the late stages of activity of the South Penninic-Austroalpine megathrust.

Acknowledgements

RB thanks for the financial support by the German National Merit Foundation, and for the financial and logistic support by the GeoForschungsZentrum Potsdam. Careful and constructive reviews by U. Ring and two anonymous reviewers are gratefully acknowledged.

References

Baumgartner, P. O. 1987. Age and genesis of Tethyan Jurassic radiolarites. *Eclogae Geol. Helv*. **80**, 831-879.

Beck, M. E. 1983. On the mechanism of tectonic transport in zones of oblique subduction. *Tectonophysics*, **93**, 1–11.

Beck Jr., M. E. 1991. Coastwise transport reconsidered: lateral displacement in oblique subduction zones, and tectonic consequences. *Phys. Earth Planet. Inter.*, **68**, 1–8.

Biehler, D. 1990. Strukturelle Eintwicklung der penninisch-ostalpinen Grenzzone am Beispiel der Arosa-Zone im Ost-Raetikon (Vorarlberg, Oesterreich). *Eclogae Geologicae Helvetiae*, **83**(2), 221-239.

Cartwright, I. & Barnicoat, A. C. (2002) Petrology, geochronology, and tectonics of shear zones in the Zermatt-Saas and Combin zones of the Western Alps. *J. Metam Geol.* **20**, 263-281.

Cliff, R. A. & Meffan-Main, S. 2003. Evidence from Rb-Sr microsampling geochronology for the timing of Alpine deformation in the Sonnblick Dome, SE Tauern Window, Austria. In: D. Vance, W. Müller and I. M. Villa *(eds.) Geochronology: Linking the Isotopic Record with Petrology and Textures, Geol. Soc. London, Special Pub.*, **220,** 159-172.

Clift, P. & Vannucchi, P. 2004. Controls on tectonic accretion versus erosion in subduction zones: Implications for the origin and recycling of the continental crust. *Reviews of Geophysics*, **42**(2), doi:10.1029/2003RG000127.

Cloos, M. & Shreve, R. L. 1988a. Subduction-channel model of prism accretion, mélange formation, sediment subduction, and subduction erosion at convergent plate margins: 1. Background and description. *Pure and Applied Geophysics*, **128**(3-4), 455-500.

Cloos, M. & Shreve, R. L. 1988b. Subduction-channel model of prism accretion, mélange formation, sediment subduction, and subduction erosion at convergent plate margins; Part II, Implications and discussion. *Pure and Applied Geophysics*, **128**(3-4), 501-545.

Deutsch, A. 1983. Datierungen an Alkaliamphibolen und Stilpnomelan aus der Südlichen Platta-Decke (Graubünden). *Eclogae Geologicae Helvetiae*, **76**(2), 295-308.

Dewey, J. F., Pitman, W. C., Ryan, W. B. F. & Bonnin, J. 1973. Plate tectonics and the evolution of the Alpine system. *Geological Society of America Bulletin* **84**, 3137-3180.

Dingeldey, C., Dallmeyer, R.D., Koller, F., & Massonne H.-J. 1997. P-T-t history of the Austroalpine nappe complex in the ‚Tarntaler Berge' NW of the Tauern Window: implications for the geotectonic evolution of the central Eastern Alps. Contrib. Mineral. Petrol. 129, 1-19.

Dürr, S. B. 1992. Structural history of the Arosa Zone between Platta and Err nappes east of Marmorera (Grisons): multi-phase deformation at the Penninic-Austroalpine plate boundary. *Eclogae Geologicae Helvetiae*, **85**(2), 361-374.

Florineth, D. & Froitzheim, N. 1994. Transition from continental to oceanic basement in the Tasna nappe (Engadine window, Graubünden, Switzerland): evidence for early Cretaceous opening of the Valais Ocean. *Schweizerische Mineralogische und Petrographische Mitteilungen*, **74**(3), 437-448.

Freeman, S. R., Inger, S., Butler, R. W. H. & Cliff, R. A. 1997. Dating deformation using Rb-Sr in white mica; greenschist facies deformation ages from the Entrelor shear zone, Italian Alps. *Tectonics*, **16**(1), 57-76.

Frey, M. & Ferreiro Mählmann, R. 1999. Alpine metamorphism of the Central Alps. In: *The new metamorphic map of the Alps; 1:500000; 1:1000000* **79; 1**. Staebli Verlag AG, Zurich, Switzerland, 135-154.

Frey, M., Hunziker, J. C., Frank, W., Bocquet, J., Dal, P. G. V., Jäger, E. & Niggli, E. 1974. Alpine metamorphism of the Alps; a review. *Schweizerische Mineralogische und Petrographische Mitteilungen* ,**54**(2-3), 247-290.

Froitzheim, N., Schmid, S. M. & Conti, P. 1994. Repeated change from crustal shortening to orogen-parallel extension in the Austroalpine units of Graubünden. *Eclogae Geologicae Helvetiae*, **87**(2), 559-612.

Froitzheim, N., Müntener, O., Puschig, A., Schmid, S. M. & Trommsdorff, V. 1996. Der penninisch-ostalpine Grenzbereich in Graubünden und in der Val Malenco. *Eclogae geol. Helv.*, **89**(1), 617-634.

Froitzheim, N., Pleuger, J., Roller, S. & Nagel, T. 2003. Exhumation of high- and ultrahigh-pressure metamorphic rocks by slab extraction. *Geology*, **31**(10), 925-928.

Gebauer, D. 1999. Alpine geochronology of the Central and Western Alps: New constraints for a complex geodynamic evolution. *Schweizerische Mineralogische und Petrographische Mitteilungen*, **79**(1), 191-208.

Glodny, J., Bingen, B., Austrheim, H., Molina, J. F. & Rusin, A. 2002. Precise eclogitization ages deduced from Rb/Sr mineral systematics: The Maksyutov complex, Southern Urals, Russia. *Geochimica et Cosmochimica Acta*, **66**(7), 1221-1235.

Glodny, J., Lohrmann, J., Echtler, H., Gräfe, K., Seifert, W., Collao, S. & Figueroa, O. 2005. Internal dynamics of a paleoaccretionary wedge; insights from combined isotope tectonochronology and sandbox modelling of the south-central Chilean forearc. *Earth and Planetary Science Letters*, **231**(1-2), 23-39.

Glodny, J., Ring, U. & Kühn, A. 2008. Coeval high-pressure metamorphism, thrusting, strike-slip, and

extensional shearing in the Tauern Window, Eastern Alps. *Tectonics,* **27***, TC4004, doi:10.1029/2007TC002193*.
Handy, M. R. 1996. The transition from passive to active margin tectonics: a case study from the Zone of Samedan (eastern Switzerland). *Geologische Rundschau,* **85**(4), 832-851.
Handy, M. R. & Oberhänsli, R. 2004. Age map of the metamorphic structure of the Alps - tectonic interpretation and outstanding problems. In: *Metamorphic structure of the Alps* (edited by Oberhänsli, R.). *Mitteilungen der Österreichischen Mineralogischen Gesellschaft*, **149**, 201-226,.
Inger, S. & Cliff, B. 1994. Dating high pressure metamorphism in the Western Alps; refining isotopic and tectonic interpretations (abstract). Eighth International Conference on Geochronology, Cosmochronology and Isotope Geology. *U.S. Geological Survey Circular*, **1107**, 149.
Kullerud, L. 1991. On the calculation of isochrons. *Chemical Geology,* **87**, 115–124.
Liu, Y., Genser, J., Handler, R., Friedl, G. & Neubauer, F. 2001. $^{40}Ar/^{39}Ar$ muscovite ages from the Penninic-Austroalpine Plate boundary, Eastern Alps. *Tectonics,* **20**(4), 526-547.
Ludwig, K. R. 1999. Isoplot/Ex Ver 2.06: a Geochronological Toolkit for Microsoft Excel. *Berkeley Geochronology Center Special Publications* **1a**.
Manatschal, G., Müntener, O., Desmurs, L. & Bernoulli, D. 2003. An ancient ocean-continent transition in the Alps: The Totalp, Err-Platta, and Malenco units in the eastern Central Alps (Graubünden and northern Italy). *Ecologae Geologicae Helvetiae,* **96**(1), 131-146.
Markley, M.J., Teyssier, C., Cosca, M.A., Caby, R., Hunziker, J.C. & Sartori, M. 1998. Alpine deformation and 40Ar/39Ar geochronology of synkinematic white mica in the Siviez-Mischabel Nappe, Western Pennine Alps, Switzerland. *Tectonics* **17**, 407-425.
Marthaler, M. & Stampfli, G. 1989. Les schistes lustrés à ophiolites de la nappe de Tsaté: un ancien prisme d'accretion issu de la marge active apulienne. *Schweiz. Mineral. Petrogr. Mitt*. **69**, 211-216.
Meffan-Main, S., Cliff, R. A., Barnicoat, A. C., Lombardo, B. & Compagnoni, R. (2004) A Tertiary age for Alpine high-pressure metamorphism in the Gran Paradiso massif, Western Alps: a Rb-Sr microsampling study. *J. Metam. Geol.* **22**, 267-281.
Müller, W., Dallmeyer, R. D., Neubauer, F. & Thöni, M. 1999. Deformation-induced resetting of Rb/ Sr and $^{40}Ar/^{39}Ar$ mineral systems in a low-grade, polymetamorphic terrane (Eastern Alps, Austria). *Journal of the Geological Society, London,* **156**(2), 261-278
Müller, W., Mancktelow, N. & Meier, M. 2000. Rb-Sr microchrons of synkinematic mica in mylonites; an example from the DAV Fault of the Eastern Alps. *Earth and Planetary Science Letters,* **180**(3-4), 385-397.
Oberhauser, R. 1983. Mikrofossilfunde im Nordwestteil des Unterengadiner Fensters sowie im Verspalaflysch des Rätikon. *Jahrb. Geol. B.-A.* **126**, 71–93.
Oncken, O. 1998. Evidence for precollisional subduction erosion in ancient collisional belts; the case of the mid-European Variscides. *Geology,* **26**(12), 1075-1078.
Pfeiffer, H.R., Colombi, A., Ganguin, J., Hunziker, J., Oberhänsli, R., & Santini, L. 1991. Relics of high-pressure metamorphism in different lithologies of the Central Alps: an updated inventory. *Schweiz. Mineral. Petrogr. Mitt.* **71**, 441-451.
Platt, J. P., Behrmann, J. H., Cunningham, P. C., Dewey, J. F., Helman, M., Parish, M., Shepley, M. G., Wallis, S. & Weston, P. J. 1989. Kinematics of the Alpine arc and the motion history of Adria. *Nature,* **337**, 158-161.
Ratschbacher, L. 1986. Kinematics of Austro-Alpine cover nappes: Changing translation path due to transpression. *Tectonophysics* **125**, 335-356.
Ratschbacher, L., Dingeldey, C., Miller, C., Hacker, B. R. & McWilliams, M. O. 2004. Formation, subduction, and exhumation of Penninic oceanic crust in the Eastern Alps; time constraints from $^{40}Ar/^{39}Ar$ geochronology. *Tectonophysics,* **394**(3-4), 155-170.
Reddy, S.M., Wheeler, J., Butler, R.W.H., Cliff, R.A., Freeman, S., Inger, S., Pickles, C., Kelley, S.P. 2003. Kinematic reworking and exhumation within the convergent Alpine orogen. *Tectonophysics* **365**, 77-102.
Ring, U., Ratschbacher, L. & Frisch, W. 1988. Plate-boundary kinematics in the Alps: motion in the Arosa suture zone. *Geology,* **16**, 696-698.
Ring, U., Ratschbacher, L., Frisch, W., Biehler, D. & Kralik, M. 1989. Kinematics of the Alpine plate-margin: structural styles, strain and motion along the Penninic-Austroalpine boundary in the Swiss-Austrian Alps. *Journal of the Geological Society, London,* **146**(5), 835-849.
Ring, U. 1989. Tectonogenesis of the Penninic/ Austroalpine boundary zone: The Arosa Zone (Grisons-Rätikon area, Swiss-Austrian Alps). *Tübinger Geowissenschaftliche Arbeiten* **Reihe A**(1), 1-177.
Ring, U., Ratschbacher, L., Frisch, W., Dürr, S. & Borchert, S. 1990. The internal structure of the Arosa Zone (Swiss-Austrian Alps). *Geologische Rundschau,* **79**(3), 725-739.
Robin, P.Y. and Cruden, A.R., 1994. Strain and vorticity patterns in ideally ductile transpressional zones.

Journal of Structural Geology, **16**, 447–466.
Rosenbaum, G. & Lister, G.S. 2005. The Western Alps from the Jurassic to Oligocene: spatio-temporal constraints and evolutionary reconstructions. *Earth-Science Reviews* 69, 281-306.
Rubatto, D., Gebauer, D. & Fanning , M. 1998. Jurassic formation and Eocene subduction of the Zermatt-Saas-Fee ophiolites: implications for the geodynamic evolution of the Central and Western Alps. *Contrib. Mineral. Petrol*. **132**, 269-287.
Schmid, S. M., Fügenschuh, B., Kissling, E. & Schuster, R. 2004. Tectonic map and overall architecture of the Alpine orogen. *Eclogae geol. Helv.,* **97**, 93-117.
Spicher, A. 1980. Tectonic map of Switzerland 1:5000 000. In: Atlas der Schweiz. Bundesamt für Landestopographie, Wabern.
Stampfli, G. & Marthaler, M. 1990. Divergent and convergent margins in the North-Western Alps. Confrontation to actualistic models. *Geodin. Acta* **4**, 159-184.
Stampfli, G. M., Mosar, J., Marquer, D., Marchant, R., Baudin, T. & Borel, G. 1998. Subduction and obduction processes in the Swiss Alps. *Tectonophysics*, **296**, 159-204
Stampfli, G. M., Borel, G. D., Marchant, R. & Mosar, J. 2002. Western Alps geological constraints on western Tethyan reconstructions. In: Rosenbaum, G. and Lister, G. S. 2002. Reconstruction of the evolution of the Alpine-Himalayan Orogen. *Journal of the Virtual Explorer*, **7**, 75 - 104.
Steiger R. H. & Jäger E., 1977, Subcommission on Geochronology: Convention on the use of decay constants in geo- and cosmochronology. *Earth Planet. Sci., Lett*., **36**, 359-362.
Thöni, M. 1981. Degree and evolution of the Alpine metamorphism in the Austroalpine Unit W of the Hohe Tauern in the light of K/Ar and Rb/Sr age determinations on micas. *Jahrbuch der Geologischen Bundesanstalt Wien,* **124**(1), 111-174.
Thöni, M. 1988. Rb-Sr Isotopic Resetting in Mylonites and Pseudotachylites: Implications for the Detachment and Thrusting of the Austroalpine Basement Nappes in the Eastern Alps. *Jb. Geol. B.-A.,* **131**(1), 169-201.
Thöni, M. 1999. A review of geochronological data from the Eastern Alps. *SMPM*, **79**, 209-230.
Trautwein, B., Dunkl, I., Kuhlemann, J. & Frisch, W. 2001. Cretaceous-Tertiary Rhenodanubian flysch wedge (Eastern Alps); clues to sediment supply and basin configuration from zircon fission-track data. *Terra Nova,* **13**(5), 382-393.
Vannucchi, P., Remitti, F. & Bettelli, G. 2008. Geological record of fluid flow and seismogenesis along an erosive subducting plate boundary. *Nature* **451**, 699-703.
Villa, I. M. 1998. Isotopic closure. *Terra Nova,* **10**(1), 42-47.
von Blanckenburg, F. & Davies, J. H. 1995. Slab breakoff: a model for syncollisional magmatism and tectonics in the Alps. *Tectonics,* **14**(1), 120-131.
von Huene, R. & Scholl, D. W. 1991. Observations at convergent margins concerning sediment subduction, subduction erosion, and the growth of continental crust. *Reviews of Geophysics*, **29**(3), 279-316.
Wagreich, M. 1991. Subsidenzanalyse an kalkalpinen Oberkreideserien der Gosau-Gruppe (Österreich). *Zentralbl. Geol. Paläontol*., **1990** II (1991), Teil I, 1645–1657.
Wagreich, M. 1993. Subcrustal tectonic erosion in orogenic belts – a model for the Late Cretaceous subsidence of the Northern Calcareous Alps (Austria). *Geology*, **21**, 941-944.
Wagreich, M. 1995. Subduction tectonic erosion and late Cretaceous subsidence along the northern Austroalpine margin (eastern Alps, Austria). *Tectonophysics,* **242**(1-2), 63-78.
Wagreich, M. 2001. A 400-km-long piggyback basin (upper Aptian-lower Cenomanian) in the Eastern Alps. *Terra Nova*, **13**(6), 401-406.
Wagreich, M. & Decker, K. 2001. Sedimentary tectonics and subsidence modelling of the type Upper Cretaceous Gosau basin (Northern Calcareous Alps, Austria). *International Journal of Earth Sciences,* **90**(3), 714-726.
Wagreich, M. & Krenmayr, H. G. 2005. Upper Cretaceous oceanic red beds (CORB) in the Northern Calcareous Alps (Nierental Formation, Austria): Slope topography and clastic input as primary controlling factors. *Cretaceous Research,* **26**(1), 57-64.
Weissert, H. J. & Bernoulli, D. 1985. A transform margin in the Mesozoic Tethys: evidence from the Swiss Alps. *Geologische Rundschau* **74**, 665-679.
Winkler, W. & Bernoulli, D. 1986. Detrital high-pressure/low-temperature minerals in a late Turonian flysch sequence of the Eastern Alps (western Austria); implications for early Alpine tectonics. *Geology* **14**, 598-601

Figures

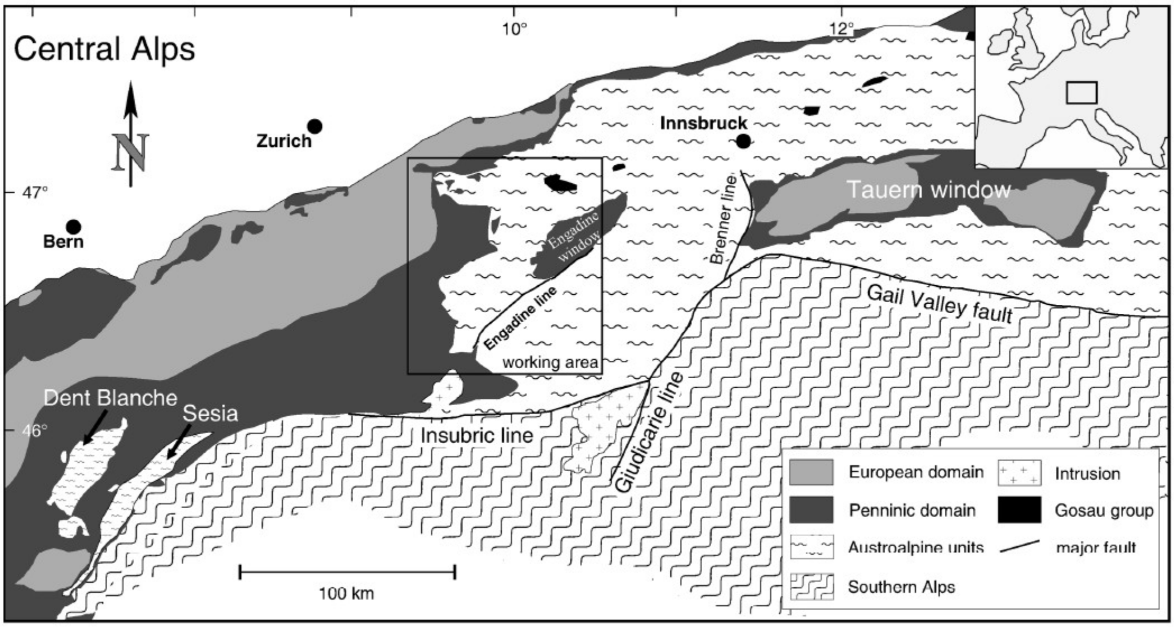

Figure 1:

Simplified geological map of the European Central Alps, modified after Frey et al. (1974) and Stampfli et al. (2002). Rectangle delineates the working area in Eastern Switzerland. The Adriatic domain comprises the Austroalpine nappe stack in the study area.

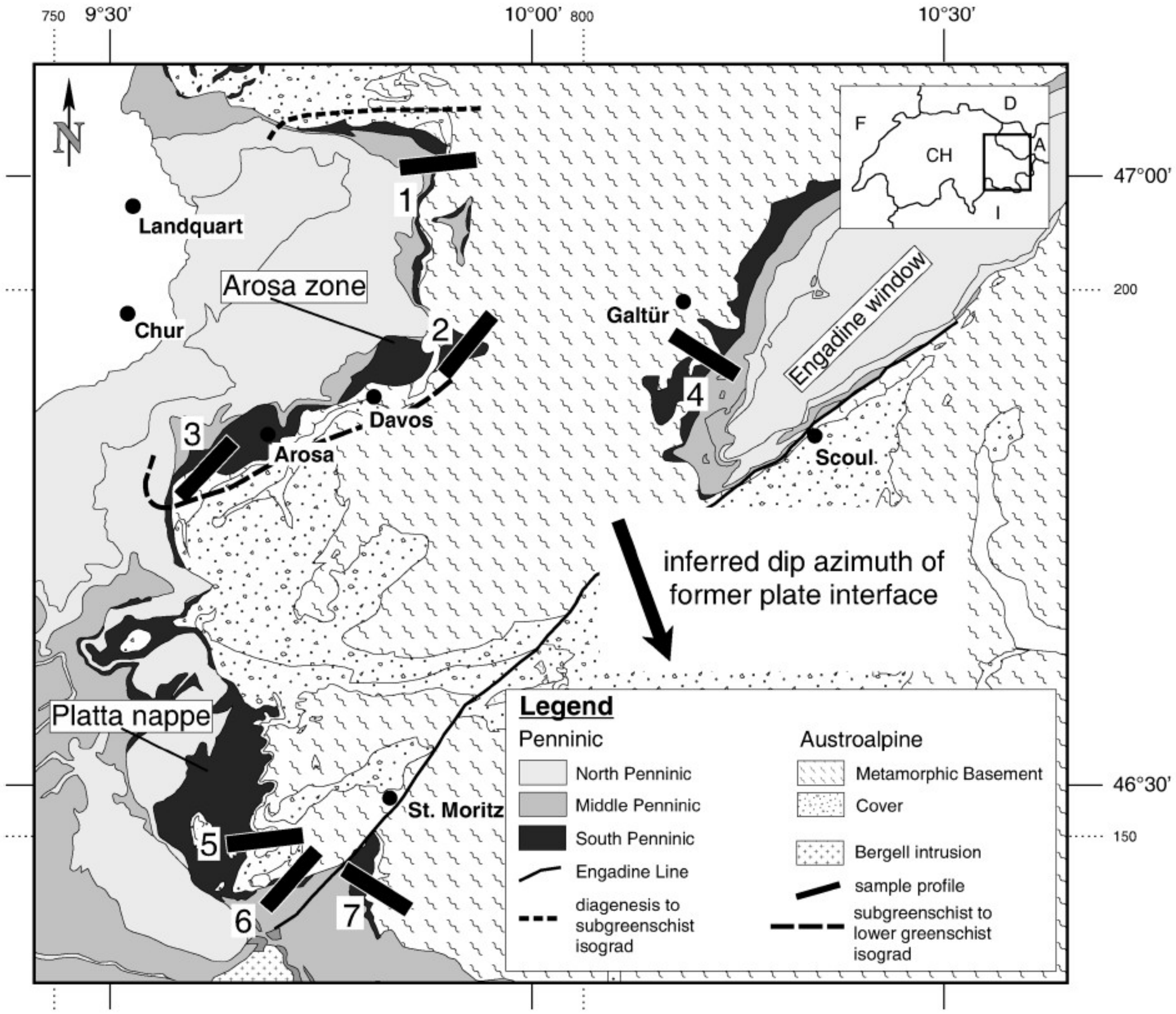

Figure 2:

Tectonic map of the study area showing the suture zone between the South Penninic (black) and the Austroalpine (dashed, part of the Adriatic plate). Black bars indicate different sampling profiles extending from domains of South Penninic origin into Austroalpine rocks. Arosa zone and Platta nappe are local names for rocks of South Penninic affinity. Based on the Tectonic map of Switzerland 1:500.000, 2nd edition (Spicher 1980).

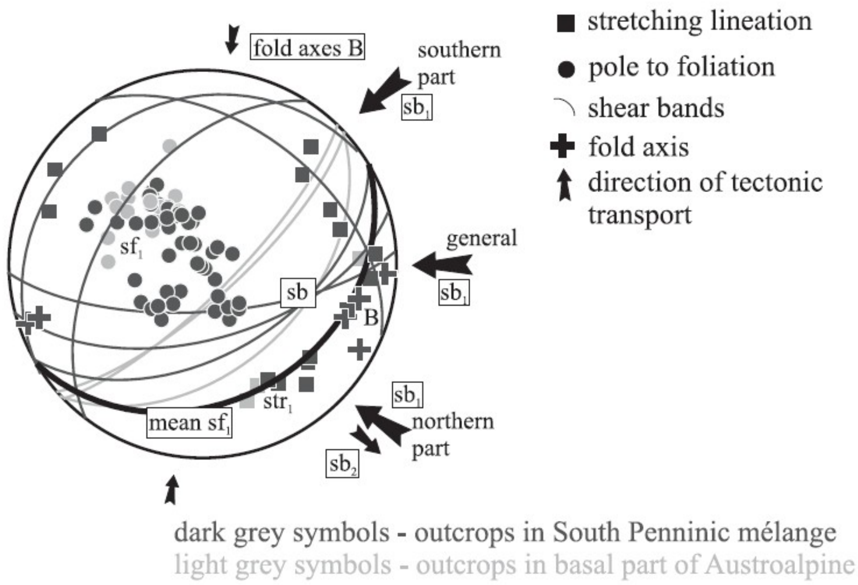

Figure 3:

Lower hemisphere, equal-area diagram of structural data of brittle-ductile to ductile deformation associated with top-NW (northern part of the working area) to top-SW (southern part of the working area) direction of tectonic transport (general top-W, large black arrows). Data are subdivided in: dark grey corresponding to outcrops located within the South Penninic mélange, light grey corresponding to outcrops located within the basal parts of the Austroalpine. In addition, subsequent non-pervasive deformation is indicated (top-SE extension and top-N thrusting, small black arrows). There is no obvious difference in the structural data obtained from outcrops in the South Penninic mélange and the Austroalpine. See text for data. str = stretching lineation, sf = foliation, B = fold axes, sb = shear bands.

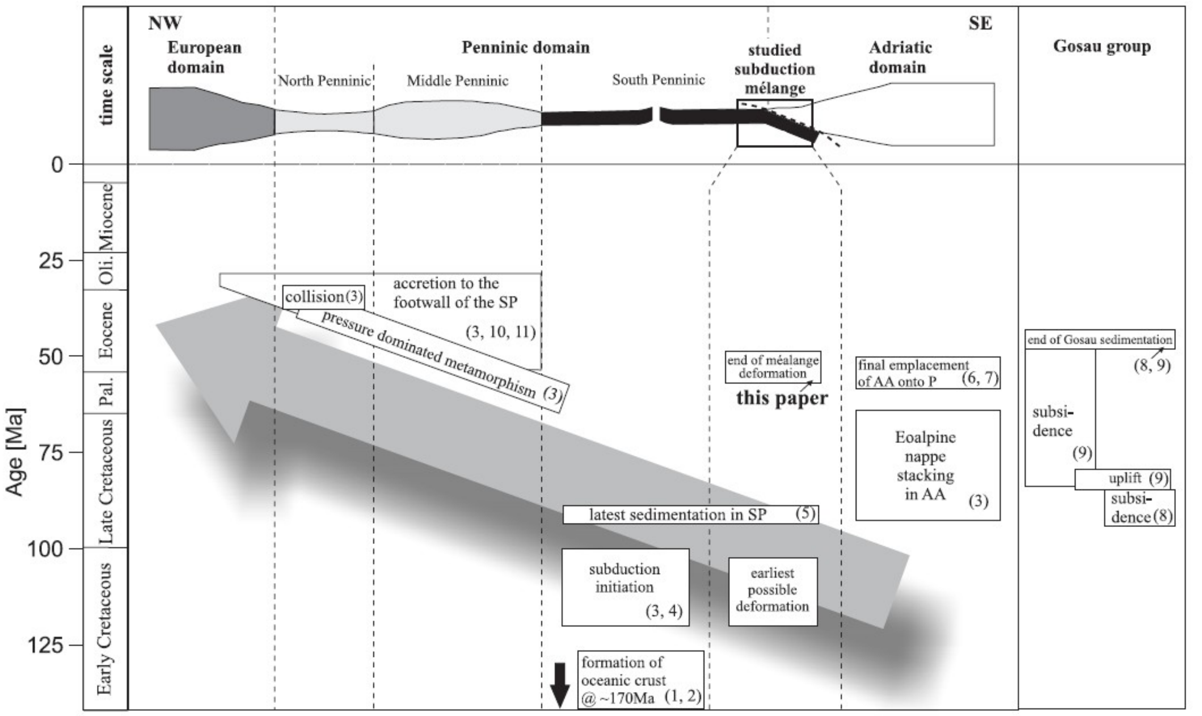

Figure 4:

Compilation of geochronological data available for the study area concerning the subduction and accretion of the South Penninic domain, deformation within the Austroalpine nappe stack, flysch deposition within the South Penninic domain and its footwall, and deformation within the Middle Penninic, North Penninic and European units. Subsidence and sedimentation history of the Gosau group is also indicated. Pale-grey arrow indicates shift in subduction-related deformation towards the foreland (i.e. towards NW). See text for details. P = Penninic;,SP, South Penninic; AA, Austroalpine; Pal, Palaeocene; Oli, Oligocene. References: (1) Gebauer (1999); (2) Ratschbacher et al. (2004); (3) Handy and Oberhänsli (2004); (4) Wagreich (2001); (5) Ring (1989); (6) Reddy et al. (2003); (7) Liu et al. (2001); (8) Wagreich (1991); (9) Wagreich 1995; (10) Markley et al. (1998); (11) Rosenbaum and Lister (2005).

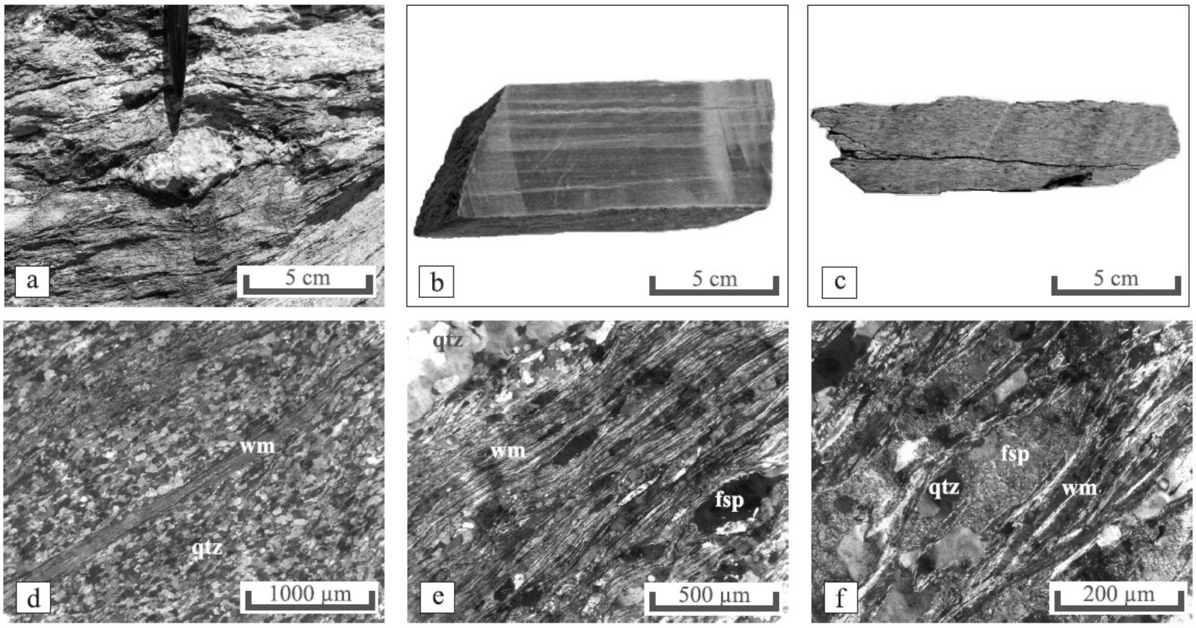

Figure 5:

Outcrop, hand specimen and thin section images illustrating different samples of the present study (a) outcrop of foliation-parallel prograde quartz mobilisate (sample B-8), (b) hand specimen of calcmylonite B-14 exhibiting tight foliation, (c) hand specimen of a quartz-rich mylonite (B-11, hanging wall), d) thin section of sample C-15 showing strong foliation expressed by the alignment of white mica (wm), (e) thin section of sample B-11 also indicating deformation-induced recrystallization of white mica in the foliation, (f) thin section of sample J91 showing heavily seriticized feldspar and incomplete dynamic recrystallization.

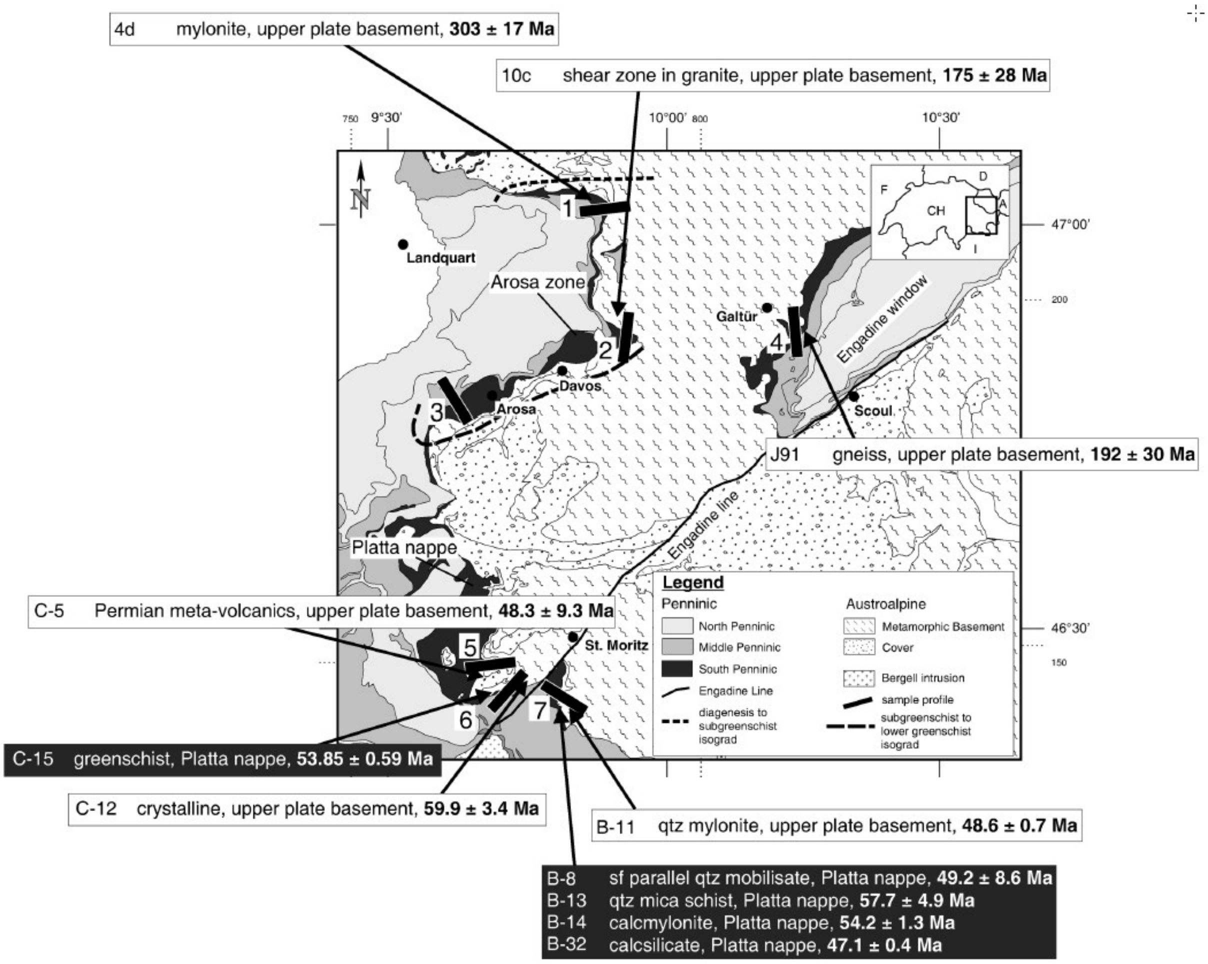

Figure 6:

Tectonic map of the working area with new Rb/Sr deformation ages for the base of Austroalpine (on white background) and the South Penninic subduction mélange (on dark background). Black bars indicate position of studied profiles across the Austroalpine-South Penninic suture. Metamorphic isogrades redrawn after Frey and Ferreiro Mählmann (1999).

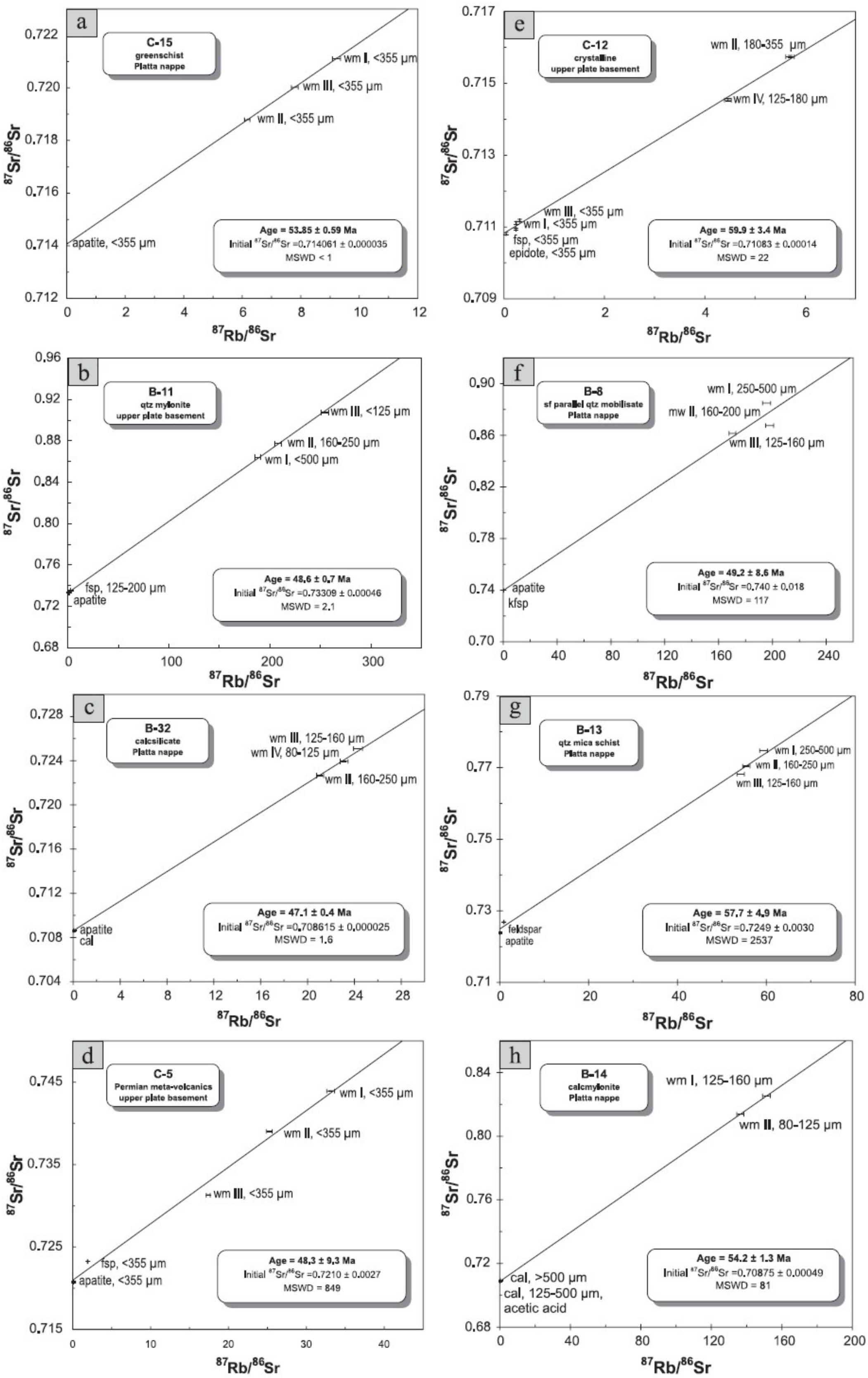

Figure 7: Rb/Sr mineral data for samples from the South Penninic mélange and the Austroalpine. Analytical data are given in Table 1. Grain size is indicated when different grain size fractions were analyzed. wm = white mica, fsp = feldspar, kfsp = K-feldspar, cal = calcite.

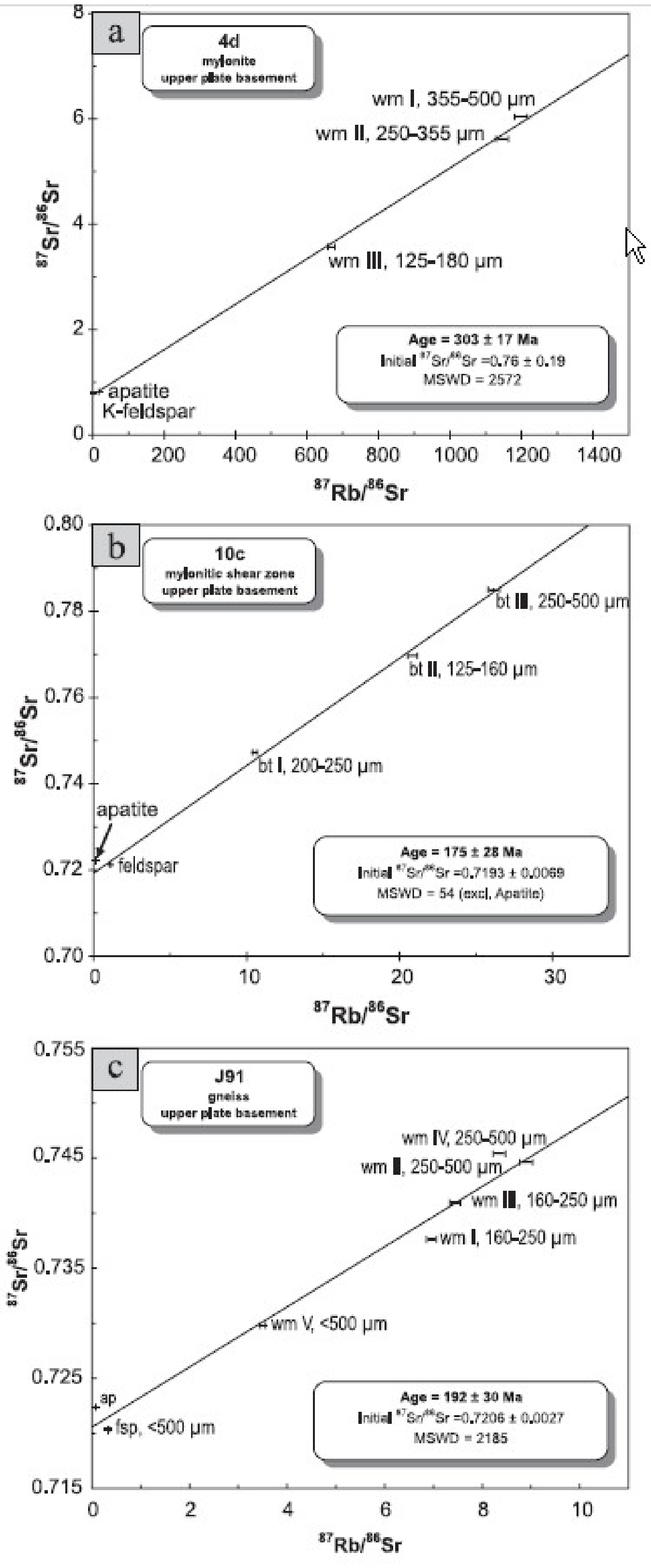

Figure 8:

Rb/Sr mineral data for samples of the Austroalpine in the northern part of the working area. Significance of isotopic disequilibria is discussed in the text. Analytical data are given in Table 1. Grain size is indicated when different grain size fractions were analyzed. Abbreviations as in Figure 7.

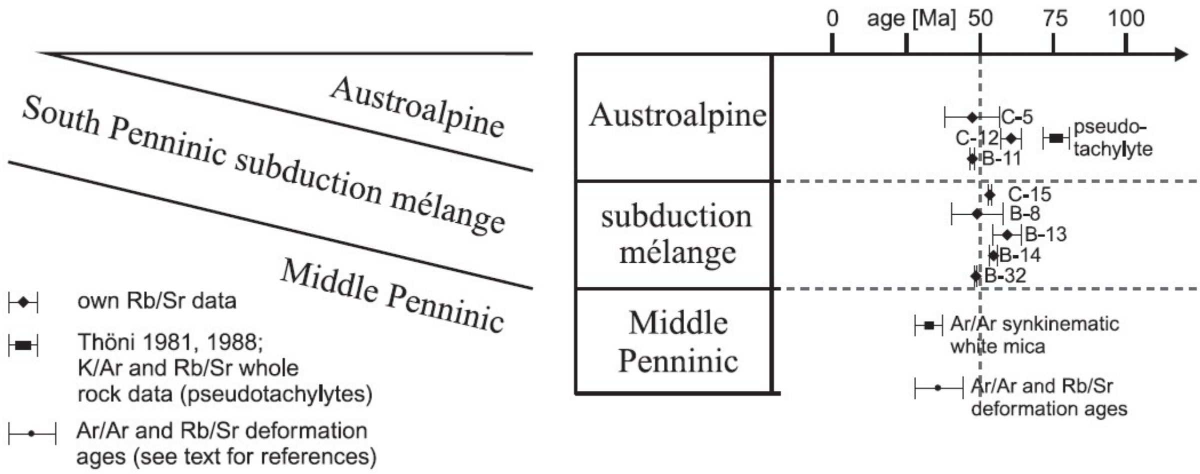

Figure 9:

Position of new Rb/Sr data relative to either the base of the hanging wall Austroalpine or the footwall South Penninic mélange, showing the similarity of deformation ages obtained for the two units.

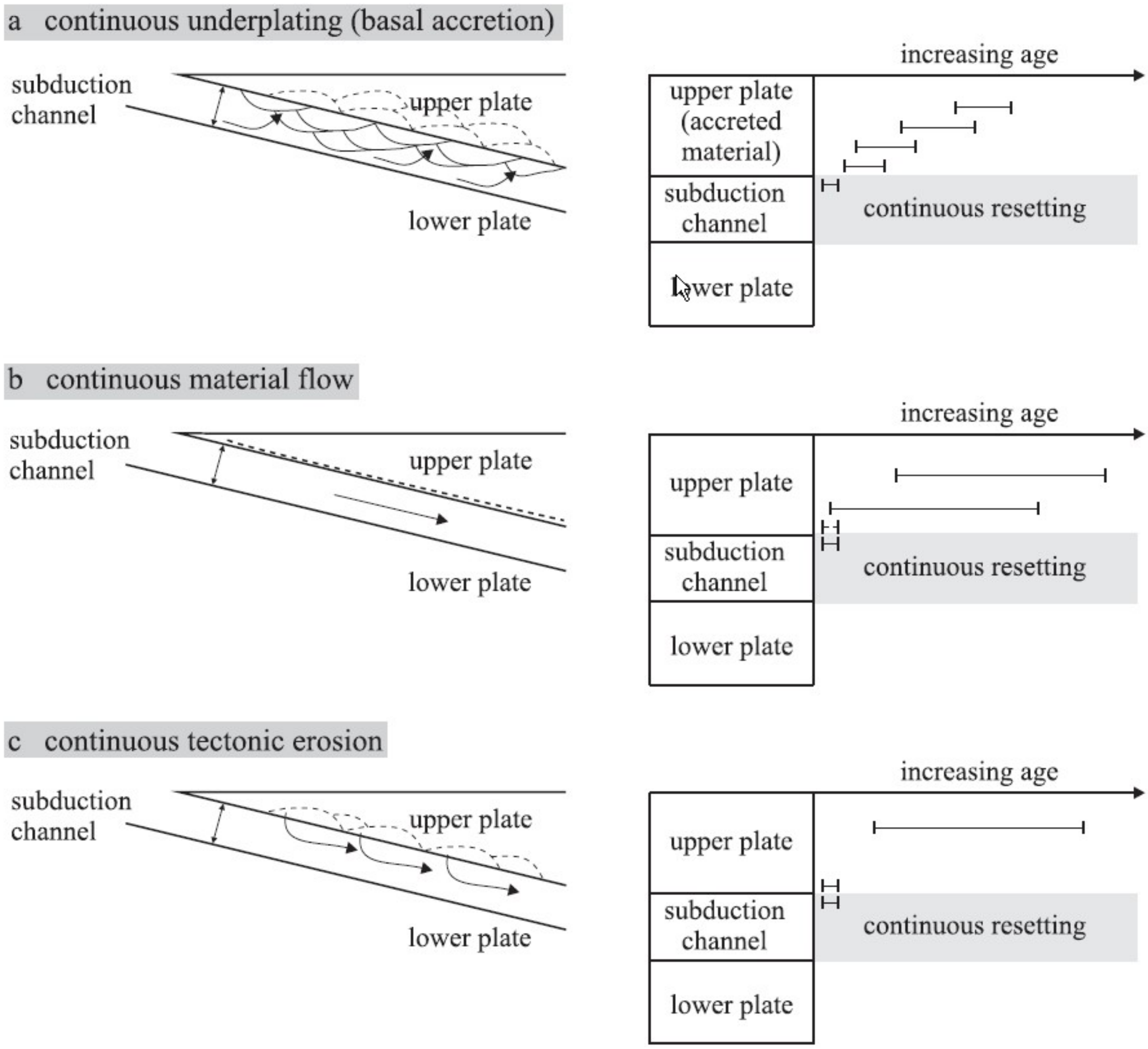

Figure 10:

Hypothetical endmember scenarios for mass transfer mode within subduction channels. a) Continuous underplating adding material to the base of the upper plate (basal accretion). Isotopic ages within the upper plate get younger towards the subduction channel. b) Steady state continuous material flow neither adding nor removing material. Clear discrepancies in isotopic ages between subduction mélange and upper plate are anticipated, controlled by the geological history of the upper plate. c) Continuous tectonic erosion removing material from the base of the upper plate. This would result in nearly identical isotopic ages for both the basal parts of the upper plate and the subduction mélange.

Tables

Table 1. *Rb/Sr analytical data*

Sample	Material, grain size (μm)	Rb (ppm)	Sr (ppm)	$^{87}Rb/^{86}Sr$	$^{87}Sr/^{86}Sr$	$^{87}Sr/^{86}Sr$ $2\sigma_m$ (%)
4d (mylonite; 303 ± 17 Ma; MSWD = 2572, Sr_i = 0.76 ± 0.19)						
PS1355	wm I, 355–500	896	3.29	1198	6.03845	0.0078
PS1354	wm II, 250–355	885	3.31	1146	5.61666	0.0050
PS1353	wm III, 125–180	783	4.35	668	3.57264	0.0116
PS1426	fsp	197	33.7	17.1	0.820349	0.0030
PS1356	apatite	9.67	91.7	0.307	0.797647	0.0018
10c (mylonite; 175 ± 28 Ma; MSWD = 54 (excl. ap), Sr_i = 0.7193 ± 0.0069)						
PS1376	bt I, 200–250	230	63.3	10.5	0.747277	0.0018
PS1375	bt II, 125–160	242	33.8	20.9	0.769687	0.0038
PS1372	bt III, 250–500	251	27.9	26.2	0.785026	0.0016
PS1374	fsp	34.4	90.7	1.10	0.721254	0.0020
PS1373	apatite	8.01	171	0.136	0.722105	0.0014
J91 (gneiss; 192 ± 30 Ma; MSWD = 2185, Sr_i = 0.7206 ± 0.0027)						
PS1511	wm I, 160–250	188	78.4	6.97	0.737618	0.0014
PS1512	wm II, 250–500	194	63.3	8.90	0.744635	0.0012
PS1513	wm III, 160–250	189	73.6	7.44	0.740965	0.0014
PS1514	wm IV, 250–500	186	64.7	8.35	0.745408	0.0014
PS1515	wm V, <500	148	122	3.51	0.729797	0.0016
PS1517	fsp, <500	70.9	599	0.343	0.720367	0.0016
PS1516	apatite	6.21	217	0.0829	0.722397	0.0018
C-5 (Permian metavolcanic rock; 48.3 ± 9.3 Ma; MSWD = 849, Sr_i = 0.7210 ± 0.0027)						
PS1505	wm I, <355	282	24.7	33.1	0.743921	0.0014
PS1506	wm II, <355	260	29.9	25.2	0.739032	0.0014
PS1507	wm III, <355	192	32.0	17.4	0.731291	0.0012
PS1510	fsp, <355	318	480	1.92	0.723244	0.0014
PS1509	apatite	12.8	312	0.119	0.720741	0.0016
C-15 (quartz mica schist; 53.85 ± 0.59 Ma; MSWD < 1, Sr_i = 0.714061 ± 0.000035)						
PS1518	wm I, <355	110	34.4	9.22	0.721113	0.0016
PS1519	wm II, <355	48.0	22.5	6.17	0.718788	0.0016
PS1520	wm III, <355	78.4	29.1	7.80	0.720022	0.0014
PS1521	apatite	10.3	3194	0.00935	0.714068	0.0018
C-12 (quartz mica schist; 59.9 ± 3.4 Ma; MSWD = 22, Sr_i = 0.71083 ± 0.00014)						
PS1490	wm I, <355	12.8	151	0.247	0.711112	0.0014
PS1491	wm II, 180–355	274	139	5.70	0.715743	0.0014
PS1493	wm III, <355	11.9	110	0.313	0.711180	0.0016
PS1494	wm IV, 125–180	179	116	4.46	0.714533	0.0014
PS1496	fsp, <355	3.42	41.3	0.239	0.710940	0.0014
PS1492	epi, <355	19.3	1318	0.0424	0.710808	0.0012
B-11 (qtz mylonite; 48.6 ± 0.7 Ma; MSWD = 2.1, Sr_i = 0.73309 ± 0.00046)						
PS1405	wm I, <500	533	8.31	188	0.864115	0.0020
PS1404	wm II, 160–250	549	7.76	208	0.877306	0.0020
PS1403	wm III, <125	557	6.45	255	0.907476	0.0030
PS1427	fsp, 125–200	27.2	27.3	2.90	0.735181	0.0062
PS1378	apatite	445	1301	0.991	0.733649	0.0012
B-8 (foliation-parallel qtz mobilizate; 49.2 ± 8.6 Ma; MSWD = 117, Sr_i = 0.740 ± 0.018)						
PS1369	wm I, 250–500	515	7.74	196	0.884915	0.0022
PS1368	wm II, 160–200	541	8.03	198	0.867532	0.0020
PS1367	wm III, 125–160	453	7.81	170	0.861505	0.0036
PS1371	kfsp, >500	4.00	55.0	0.211	0.739813	0.0014
PS1370	apatite	2.15	1157	0.00539	0.739322	0.0018
B-13 (qtz mica schist; 57.7 ± 4.9 Ma; MSWD = 2537, Sr_i = 0.7249 ± 0.0030)						
PS1409	wm I, 250–500	479	23.5	59.4	0.774758	0.0024
PS1408	wm II, 160–250	477	25.0	55.5	0.770414	0.0020
PS1407	wm III, 125–160	461	24.7	54.2	0.768190	0.0043
PS1428	fsp, 90–160	9.88	31.8	0.900	0.726888	0.0016
PS1410	apatite	6.29	1303	0.0140	0.723852	0.0014
B-14 (calcmylonite; 54.2 ± 1.3 Ma; MSWD = 81, Sr_i = 0.70875 ± 0.00049)						
PS1412	wm I, 125–160	149	2.89	151	0.825256	0.0022
PS1411	wm II, 80–125	73.4	1.57	136	0.813684	0.0062
PS1359	cc, >500	32.6	294	0.321	0.709157	0.0014
PS1377	cc, 125–500	2.06	115	0.0520	0.708628	0.0016
B-32 (calcsilicate; 47.1 ± 0.4 Ma; MSWD = 1.6, Sr_i = 0.708615 ± 0.000025)						
PS1415	wm II, 160–250	283	38.9	21.1	0.722641	0.0012
PS1414	wm III, 125–160	333	39.7	24.3	0.725086	0.0014
PS1413	wm IV, 80–125	182	22.9	23.1	0.723945	0.0014
PS1429	cc, >500	6.71	308	0.0631	0.708651	0.0016
PS1417	apatite	1.67	477	0.0101	0.708629	0.0016

An uncertainty of ±1.5% is assigned to Rb/Sr ratios. wm, white mica; fsp, feldspar; cc, calcite, bt, biotite.

Table 2. *Petrographic and (micro-)structural description of analysed samples*

Sample	Easting[1]	Northing[1]	Profile	Rock type	Tectonic unit	Analyses	qtz	fsp	ms	bt	cc	ap	epi	mgt	Remarks
4d	785310	206210	1	Mylonite	Austroalpine	Rb/Sr	× SGR	× Heavily sericitized $Ab_{50}Or_{45}An_5$	× Si p.f.u. 3.15–3.24			×			Foliation caused by alignment of ms and fsp–qtz domains; some larger fsp grains
10c	789660	193660	2	Qtz mica schist	Austroalpine	Rb/Sr	× Bulging and SGR	× Heavily sericitized $Ab_{73}An_{27}$		×		×			Tight foliation caused by alignment of bt and qtz–fsp domains; few larger bt
J91	807750	194750	4	Gneiss	Austroalpine	Rb/Sr	× SGR	× Heavily sericitized $Ab_{68}Or_9An_{23}$	× Si p.f.u. 3.12			×			Strong foliation caused by alignment of ms and qtz–fsp domains
C-5	772630	151470	5	Metavolcanic	Austroalpine	Rb/Sr	× Undulose extinction	×	×			×		×	Closely spaced foliation; ms domains partly crenulated
C-15	775380	143740	6	Qtz mica schist	South Penninic	Rb/Sr	× Partly recrystallized	×	× Si p.f.u. 3.28			×			Tight foliation caused by alignment of ms and qtz–fsp domains
C-12	776040	144510	6	Qtz mica schist	Austroalpine	Rb/Sr	× Bulging	× Almost pure ab	× Si p.f.u. 3.36				×		Some larger fsp clasts
B-11	781750	140970	7	Mylonite	Austroalpine	Rb/Sr	× SGR	× Almost pure ab	× Si p.f.u. 3.41–3.43			×			Foliation caused by alternation of ms and qtz–fsp domains
B-8	780780	142700	7	Qtz mobilizate	South Penninic	Rb/Sr	× SGR	× ab	× Si p.f.u. 3.38–3.51			×			Qtz coarse-grained
B-13	780320	142440	7	Qtz mica schist	South Penninic	Rb/Sr	×	× Almost pure ab	× Si p.f.u. 3.42–3.44			×			Strong foliation caused by alternation of qtz–fsp and ms domains; few large fsp; ms partly crenulated
B-14	780160	142840	7	Calcmylonite	South Penninic	Rb/Sr			×		× ?dol				Alternation of fine-grained and coarse-grained cc
B-32	780780	142700	7	Calcsiliate	South Penninic	Rb/Sr	× Undulose extinction		× Si p.f.u. 3.19–3.23		× With minor Fe, Mg, Mn	×			Strong foliation caused by alternation of ms, qtz and cc

SGR, subgrain rotation recrystallization; qtz, quartz; fsp, feldspar; ms, muscovite; bt, biotite; cc, calcite; epi, epidote; mgt, magnetite; dol, dolomite.
[1]Sample locations are given as Swiss grid coordinates.